2010-07

Metal-dependent inhibition of glyoxalase II: a possible mechanism to regulate the enzyme activity

Journal of Inorganic Biochemistry, New York : Elsevier, v. 104, n. 7, p. 726-731, July 2010
http://www.producao.usp.br/handle/BDPI/50150

Journal of Inorganic Biochemistry 104 (2010) 726–731

Contents lists available at ScienceDirect

Journal of Inorganic Biochemistry

journal homepage: www.elsevier.com/locate/jinorgbio

Metal-dependent inhibition of glyoxalase II: A possible mechanism to regulate the enzyme activity

Valeria A. Campos-Bermudez [a,1], Jorgelina Morán-Barrio [a], Antonio J. Costa-Filho [b], Alejandro J. Vila [a,*]

[a] IBR (Instituto de Biología Molecular y Celular de Rosario), Consejo Nacional de Investigaciones Científicas y Técnicas (CONICET), Facultad de Ciencias Bioquímicas y Farmacéuticas, Universidad Nacional de Rosario, Suipacha 531, S2002LRK, Rosario, Argentina
[b] Biofísica Molecular Sérgio Mascarenhas, Instituto de Física de São Carlos, Universidade de São Paulo, São Carlos, Brazil

ARTICLE INFO

Article history:
Received 18 August 2009
Received in revised form 15 February 2010
Accepted 9 March 2010
Available online 20 March 2010

Keywords:
Glyoxalase II
Iron
EPR
Product inhibition
Paramagnetic NMR

ABSTRACT

Glyoxalase II (GLX2, EC 3.1.2.6., hydroxyacylglutathione hydrolase) is a metalloenzyme involved in crucial detoxification pathways. Different studies have failed in identifying the native metal ion of this enzyme, which is expressed with iron, zinc and/or manganese. Here we report that GloB, the GLX2 from *Salmonella typhimurium*, is differentially inhibited by glutathione (a reaction product) depending on the bound metal ion, and we provide a structural model for this inhibition mode. This metal-dependent inhibition was shown to occur in metal-enriched forms of the enzyme, complementing the spectroscopic data. Based on the high levels of free glutathione in the cell, we suggest that the expression of the different metal forms of GLX2 during *Salmonella* infection could be exploited as a mechanism to regulate the enzyme activity.

1. Introduction

The ubiquitous glyoxalase system is composed of two metalloenzymes (glyoxalase I and glyoxalase II), whose physiological role is to catalyze the conversion of methylglyoxal to the corresponding 2-hydroxycarboxylic acids [1]. Glyoxalase I (GLX1, EC 4.4.1.5., lactoylglutathione methylglyoxal lyase) converts a thiohemiacetal (formed from methylglyoxal and glutathione) to S-D-lactoylglutathione (SLG), while glyoxalase II (GLX2) takes the latter as a substrate and catalyzes its hydrolysis to yield D-lactic acid and glutathione (GSH) [2,3] (Fig. 1A).

Although GLX2 is able to hydrolyze many different glutathione thioesters, S-D-lactoylglutathione (SLG) is the preferred substrate for this enzyme from most sources including human, yeast, and plants. The glyoxalase enzymatic system is essential for chemical detoxification, and therefore has been identified as a target for the development of anti-cancer and anti-protozoan drugs [4–6].

GLX2 belongs to the metallo-β-lactamase superfamily, which is characterized by an αβ/βα fold containing a conserved motif able to bind up to two metal ions in their active sites. Most hydrolases from this superfamily use Zn^{II}, a redox inactive metal ion for their roles, such as metallo-β-lactamases [7,8], N-acyl homoserine (AHL) lactonases [9,10] and tRNAseZ [11], whereas the terminal oxidase rubredoxin: oxygen oxidoreductase (ROO) from *D. gigas* contains a binuclear iron site [12–14]. GLX2, despite exhibiting the same coordination sphere displayed by other hydrolases from this superfamily (Fig. 1B), has been an outstanding exception regarding the metal ion dependence with different metal cofactors [15–20].

In general, the wild type forms of the recombinant GLX2 isoenzymes characterized up to now were isolated with varying amounts of iron, zinc and manganese bound to their active sites [15–20]. Surprisingly, the different metal derivatives show comparable high catalytic efficiencies [15–20]. An exception to this observation is human GLX2, which has been reported to be inactive in its Mn-bound form [20]. Despite the existence of three crystallographic structures (2QED, 1QH5, 1XM8) [18,19,21] which have been refined with different metal ions in its active sites, this puzzling promiscuity has precluded the identification of the native metal ion in GLX2.

Most mechanistic proposals so far have considered exclusively the di-Zn^{II} derivative, based on crystallographic, kinetic and spectroscopic studies, and (more recently) theoretical calculations at the quantum level [17,21,22] (Fig. 1B). However, one may argue whether this mechanism could be general to all metal derivatives.

Here we report a spectroscopic and kinetic study on GloB, the glyoxalase II from *Salmonella typhimurium* [19], upon addition of substrate S-D-lactoylglutathione (SLG) or the product glutathione (GSH). We have interrogated the enzyme purified from rich medium, containing mixed metallic centers, as well as Fe-, Zn- and Mn-enriched forms [19]. We have found that GloB is differentially inhibited by

* Corresponding author. Fax: +54 341 4390465.
E-mail addresses: campos@cefobi-conicet.gov.ar (V.A. Campos-Bermudez), moran@ibr.gov.ar (J. Morán-Barrio), ajcosta@if.sc.usp.br (A.J. Costa-Filho), vila@ibr.gov.ar (A.J. Vila).
[1] Present address: CEFOBI (Centro de Estudios Fotosintéticos y Bioquímicos), Consejo Nacional de Investigaciones Científicas y Técnicas (CONICET), Facultad de Ciencias Bioquímicas y Farmacéuticas, Universidad Nacional de Rosario, Suipacha 531, (S2002LRK), Rosario, Argentina.

0162-0134/$ – see front matter © 2010 Elsevier Inc. All rights reserved.
doi:10.1016/j.jinorgbio.2010.03.005

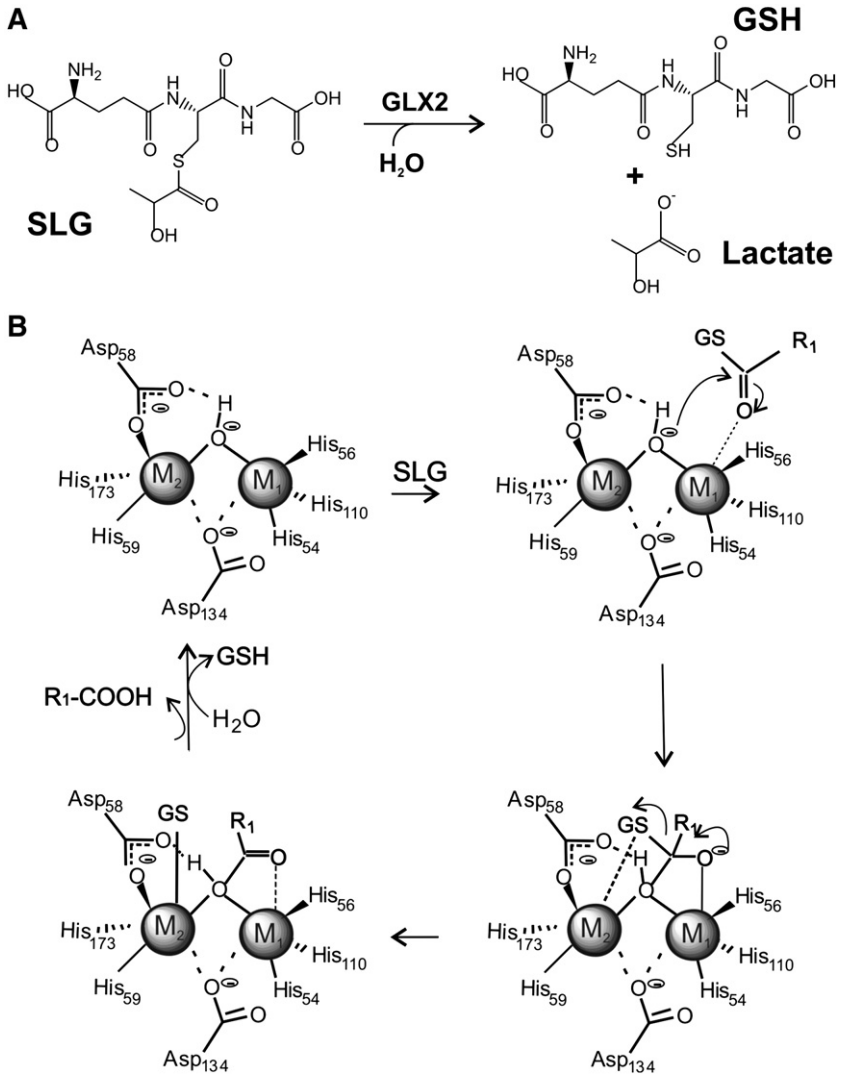

Fig. 1. (A) Reaction catalyzed by glyoxalase II (GLX2). (B) Proposed reaction mechanism for dimetallic-GLX2 based on crystallographic, kinetic and theoretical calculations. The metal ion bound to 3 His residues (M1) is proposed to deliver the attacking nucleophile, while the M2 site favors S–C bond cleavage by stabilizing the negative charge in the sulfur atom of the glutathione moiety.

glutathione depending on the bound metal ion, and we provide a structural model for this inhibition mode.

2. Experimental procedure

2.1. General

S-D-lactoylglutathione (SLG) was purchased from Sigma-Aldrich. All chromatographic steps were performed in an Amersham Biosciences liquid chromatography system operating at 4 °C. Metal standards were purchased from Fisher Scientific and were diluted with distilled water. All other chemicals used in this study were purchased commercially and were of the highest quality available.

2.2. Protein overexpression and purification

GLX2 (GloB) from *S. typhimurium* 14028s recombinantly produced in *E. coli*, was used for this study. Protein overexpression and purification were performed using the pET32-gloB vector, as previously described [19]. Fractions with GLX2 activity were pooled and dialyzed against 10 mM 4-morpholinepropanesulfonic acid (MOPS) 0.2 M NaCl at pH 7.2. In order to selectively produce metal-enriched enzyme forms, minimal media M9 was employed in culture growth supplemented with metal ions from stock solutions of $Fe(NH_4)SO_4$, $MnCl_2$, or $ZnCl_2$, to reach a final concentration of 100 μM in the culture. The minimal media contained 4 g/L D-(+)-glucose (Sigma), 12.8 g/L $Na_2HPO_4 \cdot 7H_2O$, 3 g/L KH_2PO4, 0.5 g/L NaCl, 1.0 g/L ammonium sulfate, 10 μM $CaCl_2$ and 1 mM $MgSO_4$. The metal ions were added in the moment of induction, when the growth cultures reached an OD_{600} of 0.6–0.8. The purification protocol is described in Ref. [19]. Thus, we obtained the iron-enriched GloB (FeGloB), manganese-enriched GloB (MnGloB) and zinc-enriched GloB (ZnGloB).

2.3. Protein concentration

Enzyme concentration was determined by measuring the $A_{280\,nm}$ and using the extinction coefficient $\varepsilon_{280\,nm} = 28{,}030\ M^{-1}\ cm^{-1}$ [19]. This parameter was calculated from amino acid composition information by applying a modified Edelhoch method [23].

2.4. Metal analysis

The metal content of the GloB samples was measured using atomic absorption spectroscopy in a Metrolab 250 AA instrument. Purified

enzymes were diluted with 10 mM MOPS pH 7.2, to a concentration of 30 μM and analyzed for zinc, manganese and iron. The metal content of GloB produced in minimal medium was the following: FeGloB: 0.86 ± 0.02 eq iron, 0.05 ± 0.02 eq manganese and 0.04 ± 0.01 eq zinc; MnGloB: 0.04 ± 0.01 eq iron, 0.81 ± 0.06 eq manganese and 0.04 ± 0.01 eq zinc; ZnGloB: 0.08 ± 0.01 eq iron, 1.42 ± 0.01 eq zinc and manganese was not detected. The metal content data presented in this paper represent an average from at least three preparations of each growth condition.

2.5. ^{1}H NMR spectroscopy

NMR spectra were recorded in a Bruker Avance II 600 spectrometer operating at 600.13 MHz. ^{1}H NMR spectra were recorded under conditions to optimize detection of the fast-relaxing paramagnetic resonances, either using the superWEFT pulse sequence [24,25] or water presaturation. Spectra were acquired over large spectral widths with acquisition times ranging from 16 to 80 ms, and intermediate delays from 2 to 35 ms. 1D experiments with solvent presaturation were used to record isotropically shifted signals closer to the diamagnetic envelope. The samples were loaded into Wilmad 5-mm NMR tubes. The substrate or product was prepared as 100 mM stock solutions in 100 mM MOPS at pH 7.2 (pD 6.8). A final 1:10 enzyme to reactant ratio was used to record the spectra in presence of the adducts.

2.6. Electron paramagnetic resonance spectroscopy

X-band (9.5 GHz) EPR spectra were measured on a Bruker ELEXSYS E580 system (Bruker BioSpin, Germany) at 4.7 K. The temperature was controlled with an Oxford ITC503 cryogenic system. EPR samples containing a convenient amount of protein or the protein to which the substrate or product were added (up to a 1:10 ratio) were frozen by immersion in liquid nitrogen and then placed in the spectrometer rectangular cavity. All EPR data were corrected by subtracting a baseline corresponding to the EPR signal of the buffer. Other acquisition conditions: modulation amplitude, 1 mT; modulation frequency, 100 kHz; microwave power, 4 mW. A typical EPR sample was 1 mM in 10 mM MOPS pH 7.2 buffer.

2.7. UV–visible spectroscopy

Spectra of GloB samples in the absence and presence of substrate or product in different ratios, were recorded between 240 and 800 nm at 25 °C in a Jasco 550 UV–vis spectrophotometer in quartz cuvette of 1 cm of path length. Differential spectra were obtained by subtracting the spectrum of the enzyme in its unbound form. Typical samples of GloB containing different metal ions were up to 1 mM in protein, while the spectra of Fe-enriched, Mn-enriched and Zn-enriched were recorded on samples typically *ca.* 30 μM.

2.8. End product inhibition studies of SLG hydrolysis

Inhibition studies were performed on selectively metal-enriched GloB using glutathione, one of the products of SLG hydrolysis. Steady state kinetic studies of purified GloB variants in the presence of varying concentrations of GSH (0.2 to 5 mM) were conducted by measuring the rate of hydrolysis of a fixed concentration of SLG (400 μM) at 240 nm ($\varepsilon_{240} = 3100\ M^{-1}\ cm^{-1}$). A glutathione stock solution was prepared in 100 mM MOPS, pH 7.2. The enzyme (400 nM) and inhibitor were incubated, and then the substrate was added. IC_{50} values were determined by fitting the data of initial rates to the following equation: $(1 - v_i/v_o) * 100 = \text{Imax.}[I]/(IC_{50} + [I])$. Measurements were performed at least by triplicate in a reaction volume of 1 ml of 10 mM MOPS, 0.2 M NaCl pH 7.2 buffer, at 30 °C in a Jasco 550 UV–vis spectrophotometer.

3. Results

GloB was obtained as previously described in Campos-Bermudez et al. [19]. The typical metal content of enzyme samples expressed in rich medium is 0.2 zinc; 0.6 iron and 0.3 manganese per protein. Selectively metallated variants were produced by expressing the protein in minimal medium adequately supplemented with the required metal ion. The behavior of these proteins upon the addition of substrate or product was analyzed by different spectroscopic techniques.

3.1. Electron paramagnetic resonance

The EPR spectrum of resting-state GloB recorded at 4.7 K (Fig. 2A) disclosed the coexistence of different paramagnetic species. As already shown, the different observed signals can be assigned on the basis of spectral simulations [19]. The main components in the EPR spectra are due to two different iron centers. Resonances at $g_{eff} \sim 4.3$ and 9.1 are characteristics of magnetically isolated high-spin Fe^{III} in a rhombic environment [15,18,19,26–28]. The broad feature at $g < 2$ corresponds to an antiferromagnetically coupled dinuclear center which involves a high-spin ($S = 5/2$) Fe^{III} ion and a high-spin ($S = 2$) Fe^{II} ion [15,18,19,28]. The six-line pattern centered around $g = 2.0$ is due to Mn^{II} bound to the active site (Fig. 2A).

S-D-lactoylglutathione (SLG, the enzyme substrate) was added to GloB, and the EPR spectrum was recorded after manual mixing and sample freezing. The spectrum (Fig. 2B) revealed changes in the resonances stemming from the iron centers at $g_{eff} \sim 4.3$, 9.1 and <2, while the signals arising from the Mn^{II} site could be accounted for in the simulation by the same set of parameters obtained for resting-state GloB, suggesting that the Mn^{II} ions are not perturbed. Addition of glutathione (GSH, a reaction product), gave rise to similar changes on the EPR signals corresponding to the iron centers, while those from the Mn^{II} sites also remained unperturbed (Fig. 2C).

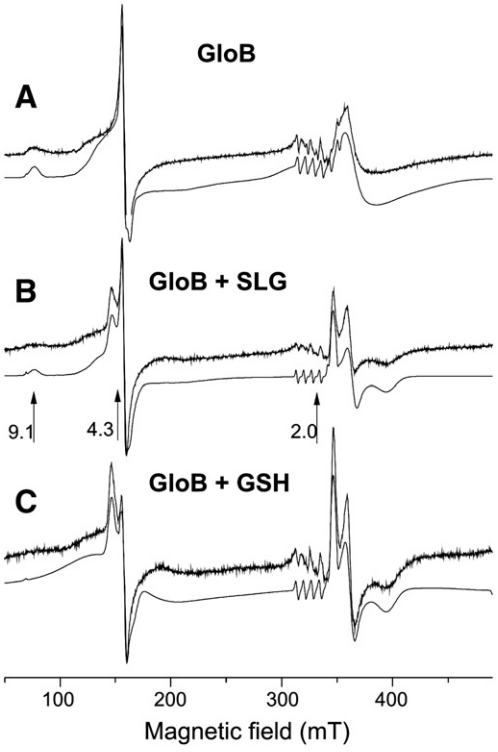

Fig. 2. Experimental (upper traces) and calculated (lower traces) X-band EPR spectra of 1 mM GloB (A) as isolated; (B) after the addition of SLG and (C) after the addition of GSH. The spectra were recorded at 4.7 K and simulated as described in the text. The arrows indicate approximate *g*-values.

Analysis of the individual features revealed that in the presence of SLG or GSH, the uncoupled signal (g_{eff}~4.3) presented higher zero-field splittings ($D = 0.55\ cm^{-1}$ and $E/D = 0.285$) compared to resting-state GloB ($D = 0.33\ cm^{-1}$ and $E/D = 0.195$). The increase in D-values can be attributed to a change in the coordination sphere of the iron ion, with more electron-donating atoms; while the higher E/D ratio reveals a larger rhombicity in the Fe^{III} center. Both parameters are consistent with the binding of an additional ligand to the Fe^{III} ion [29,30].

Regarding the signal accounting for the coupled center ($g<2$), the addition of either SLG or GSH led to lineshape and g-value differences (Fig. 2B–C), revealing that the environment of the binuclear center is significantly perturbed in both cases. Spectra of coupled centers are very sensitive to changes in the coordination environment of the binuclear site which can be reflected in the magnitude of the super-exchange coupling (J) between the metal centers, and the zero-field splittings (D) of each ion, among other features [31–34]. Effective g-values for these systems could be easily determined assuming an $S = 1/2$ spin system and yielded, in the presence of ligands, 1.95, 1.87, and 1.71 ($g_{av} = 1.84$). Thus, the addition of exogenous ligands (SLG or GSH) is reflected as a significant increase in g_{av} value for GloB in the presence of ligands ($g_{av} = 1.84$) as compared to pure GloB ($g_{av} = 1.76$), which suggests a stronger coupling regime upon ligand binding.

The EPR spectra of Fe-enriched GloB before and after addition of substrate (SLG) or product (GSH) revealed the same spectral features that for the heterogeneous sample of GloB (not shown). The spectra disclosed mononuclear and binuclear Fe centers, and a weak six-line pattern. Double-integration of the spectra showed that this six-line pattern is responsible for less than 5% of the total signal intensity, indicating that this is the result of a very minor contribution from Mn centers in the sample, which is in agreement with metal analyses. The spectra showed that addition of substrate (SLG) or product (GSH), led to the same spectral alterations that those observed in Fig. 2B–C.

3.2. ^1H nuclear magnetic resonance

The ^1H NMR spectrum of GloB was recorded under conditions tailored to optimize detection of the fast-relaxing signals close to the paramagnetic metal center [25]. The spectrum of GloB reveals a set of hyperfine-shifted signals attributed to the His and Asp ligands of the metal site (Fig. 3) of a weakly antiferromagnetic coupled Fe^{III}/Fe^{II} system. Resonances corresponding to an uncoupled Fe^{III} center cannot be detected, since considerably broader lines are expected [35]. The addition of excess substrate (SLG) to GloB, resulted in a new set of resonances sharper than those from the resting-state enzyme (Fig. 3B). Addition of GSH to GloB rendered a spectrum very similar to that resulting upon substrate addition (Fig. 3C). Since NMR spectra are recorded at room temperature, in contrast with EPR, and NMR acquisition times are rather long (in relation with the GloB $k_{cat} = 170\ s^{-1}$), the time stability of the monitored species suggests that all studied spectra correspond to an enzyme–product adduct. We must recall that the glutathione moiety is present both in the substrate and product molecules (Fig. 1A).

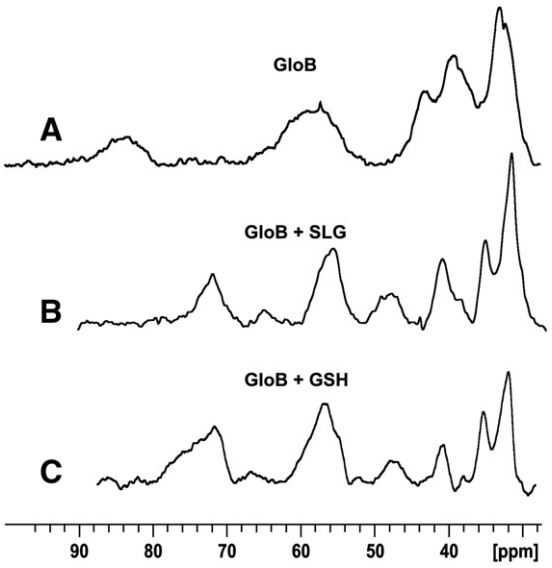

Fig. 3. ^1H NMR spectra of GloB (A) as isolated, (B) after the addition of SLG and (C) after the addition of GSH. The spectra were recorded at 600 MHz, pH 7.2, and 298 K in 10 mM MOPS buffer, 0.2 M NaCl.

3.3. UV–vis spectroscopy

To test the hypothesis that the formed species is an enzyme–product complex, the interaction of GloB with SLG and GSH was followed by UV–vis spectroscopy. We initially attempted these experiments with a sample of GloB obtained from expression in rich media, containing Fe, Zn and Mn. The addition of excess SLG resulted in the appearance of a blue color, corresponding to an absorption band centered at 590 nm, with an estimated extinction coefficient of $300\ M^{-1}\ cm^{-1}$ (Fig. 4A). This spectral feature vanished after several hours, confirming the formation of a stable adduct with the enzyme. This feature is in good agreement with the presence of a ligand-to-metal charge transfer (LMCT) band of a Cys ligand to a high-spin Fe^{III} in an octahedral coordination, reminiscent of those observed in superoxide reductase and model complexes [36–38]. An additional intense band at 320 nm is observed in the differential spectrum (Fig. 4A), which can be assigned to a (Cys)S–Fe^{II} LMCT [38]. Similar UV–vis specta were obtained for Tflp, a ferredoxin-like protein from *Thermoanaerobacter tengcongensis* [39] belonging to the metallo-β-lactamase superfamily, where a disulfide bond is near the di-Fe center in the active site.

When GSH was added to GloB, the same spectral features were observed (Fig. 4A). These results further confirm that the spectra

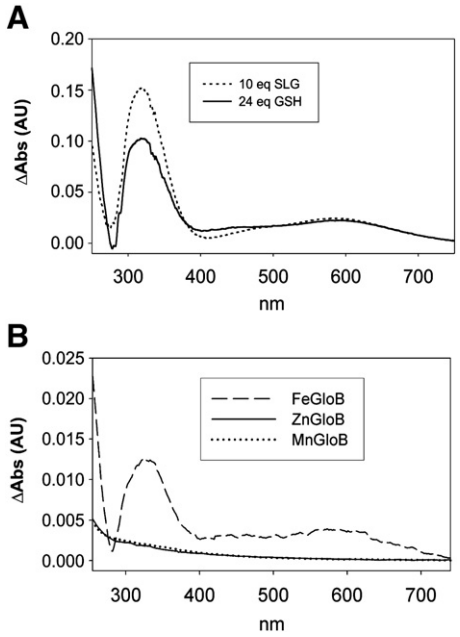

Fig. 4. Differential UV–visible spectrum of GloB produced in rich medium after the addition of substrate or product (A) and from minimal medium supplemented either with Fe^{II} (FeGloB), Mn^{II} (MnGloB) or Zn^{II} (ZnGloB) after the addition of 10 equivalents of substrate SLG (B). The differential spectra were obtained by subtracting the spectrum of unbound GloB. The observed features are in good agreement with the presence of a ligand-to-metal charge transfer (LMCT) band of a Cys ligand to iron ions.

recorded after addition of SLG correspond to a stable enzyme–product (E–P) adduct, formed as the result of the interaction of the metal site with the Cys-containing glutathione moiety of the substrate (Fig. 1A). These data are consistent with the crystal structure of the human enzyme complexed with GSH (1QH5), in which the sulfur atom of this Cys residue is at 2.86 Å from one of the metal ions [21]. The absorption feature at 590 nm observed for the GloB–GSH complex displays a relatively low extinction coefficient, which is consistent with the relatively long S–Fe^{III} bond reported in the crystal structure. The lack of a spectral feature at 280 nm allows us to discard the presence of a Cys–Mn^{II} LMCT, *i.e.*, confirming that this adduct is exclusively formed by the iron form of GLX2 [36].

When the same experiments were performed in the Fe-enriched form, obtained by expression in minimal medium supplemented with Fe^{II}, we observed the same LMCT bands upon addition of either SLG or GSH. These experiments unequivocally confirm that the features observed in the mixed GloB sample correspond to the iron form. Instead, when similar titrations were conducted in the Mn-enriched and Zn-enriched forms of GloB, no distinctive features could be detected in the differential spectra even upon addition of a 10-fold excess of the exogenous ligands up to 240 nm (Fig. 4B). Minor changes in the spectra can be attributed to alterations in the absorption features of the aromatic residues, as results from the fine structure of the differential spectra. These data allow us to discard the formation of a Cys–Mn^{II} CT band, which is expected to appear at 280 nm. This is validated by comparison with the spectrum obtained with the Zn form of the enzyme, which it is not expected to exhibit a LMCT in this spectral range.

3.4. Product inhibition of the specific metallated forms

The differential behavior of the different metallated forms towards the formation of enzyme–product complexes led us to analyze product inhibition of each metal form of GloB. We obtained the Mn-enriched, Zn-enriched and Fe-enriched forms of GloB, by expression in minimal medium as already described [19], and we tested their inhibition by glutathione. Fe- and Zn-GloB were inhibited at submillimolar concentrations of glutathione, while the IC_{50} value for Mn-GloB is 1.5 mM. These results are in agreement with the spectroscopic data, which show strong product binding to the iron-substituted enzyme, and not to the manganese forms. These data also reveal that the behavior of the Zn form resembles that of Fe-GloB.

4. Discussion

Glyoxalase II belongs to the metallo-β-lactamase superfamily, which includes several zinc-dependent hydrolases, such as metallo-β-lactamases, endonuclease tRNase Z, AHL lactonase and phosphorylcholine esterase [40]. GLX2 is an exception in that different metal derivatives show sizably high catalytic performances for most isoforms [15–20]. This is valid for the plant and bacterial isozymes characterized so far, since, despite high sequence homology, human GLX2 is inactive in its Mn^{II} form [20]. This fact suggests that metal discrimination could play a role in glyoxalase activity.

The proposed mechanism for the di-Zn enzyme assumes binding of S-D-lactoylglutathione substrate to the enzyme, mainly by recognition of the glutathione moiety by active site residues, excluding a direct interaction with the metal ion (Fig. 1B) [22]. The metal ion bound to 3 His residues (M_1) is proposed to deliver the attacking nucleophile, at the same time stabilizing the development of negative charge in an oxygen atom during formation of a tetrahedral intermediate. After the nucleophilic attack, the M_2 site favors S–C bond cleavage by stabilizing the negative charge in the sulfur atom of the glutathione moiety. After protonation and bond cleavage, a lactate and a glutathione moiety remains bound to the M_1 and M_2 ions, respectively (Fig. 1B). A sequential mechanism for product release has been proposed [17,21,22].

Here we report a metal-selective product inhibition, which allow us to obtain some mechanistic insights. By using complementary spectroscopic techniques, we provide evidence supporting that: (1) addition of either substrate (SLG) or product (GSH) to GloB results in the formation of a stable enzyme–product (GloB–GSH) complex; (2) this adduct is formed by the iron variants of the enzyme, and not by the manganese derivatives; (3) a thiol–Fe bond is formed between the Cys moiety of GSH and the metal site; and (4) the dinuclear iron sites show an enhanced antiferromagnetic coupling in the GloB–GSH adduct.

The finding of a stable thiol–Fe bonding interaction can be readily attributed to product inhibition by glutathione, supporting a sequential, ordered mechanism for product release after hydrolysis [17,21,22]. The reported lower K_I for glutathione suggests that it is bound more tightly to the active site and therefore is released after D-lactic acid [17].

EPR spectroscopy reveals that the coupling between the two iron ions is stronger in the enzyme–product complex. This coupling is expected to occur by involving Asp127 as a bridging ligand (Fig. 5). One possible rationale for this observation is to assume an equilibrium between the bridged and non-bridged forms in the free enzyme, which is consistent with the variable geometries observed in different crystal structures [15,18,19,21], that would be shifted towards the bridged one upon formation of the EP adduct (Fig. 5A). Sharing the Asp127 ligand between the two metal ions upon thiolate binding may compensate the increase in negative charge in the metal coordination sphere. Another possibility is that the sulfur atom from glutathione forms a strong hydrogen bond to the bridging hydroxide, thus imparting more oxo character in the bridging unit, giving rise to a stronger coupling.

Finally, we could also assume that the thiolate group of glutathione is bound to the metal site bridging the two iron ions (Fig. 5B), in a position equivalent to the one occupied by the nucleophile in the resting-state enzyme. The GloB–GSH complex displays S–thiol–Fe^{III} and S–thiol–Fe^{II}: CT bands (Fig. 4). This observation could be accounted for by assuming a bridging glutathione moiety, confirming again that product release is ordered in a sequential fashion.

The most relevant observation regarding this enzyme–product complex concerns its metal selectivity. Mn^{II}–thiolate bonds are less covalent and weaker than iron–thiolate bonds, providing a rationale for this differential behavior [36]. This is also consistent with the finding that, in general, the Mn^{II} forms of different GLX2s are the most efficient ones [15,16,19,41].

Fe^{II} and Mn^{II} are regarded as the most important transition metal ions involved in host–bacterial pathogen interactions [43]. The acquisitions of both metal ions, and particularly Mn^{II}, are required for intracellular survival and replication of *Salmonella enterica* serovar *typhimurium* in macrophages *in vitro* and for virulence *in vivo* [44,45]. Thus, fine regulation of metal ions availability *in vivo* could determine the pathogen survival inside host cells. Since the levels of free glutathione *in vivo* are high, this differential inhibition mode might be taken as an indication that Mn^{II} is the native metal ion, in line with our results. However, additional experimental work is needed to state that.

The glyoxalase system in *Salmonella* strains is the main defense mechanism to the accumulation of methylglyoxal generated in the phagolysosome during infection [42]. In contrast to other genes involved in methylglyoxal detoxification, that are induced in the *Salmonella*-containing vacuole during infection (such as those coding GLX1), the expression levels of *gloB* are constant through the pathogen infection cycle [42]. Based on the evidence herein presented that shows that inhibition by GSH is metal-dependent, the assembly of a specific metal-enriched form of GLX2 could be exploited as a mechanism to regulate the enzyme activity *in vivo*.

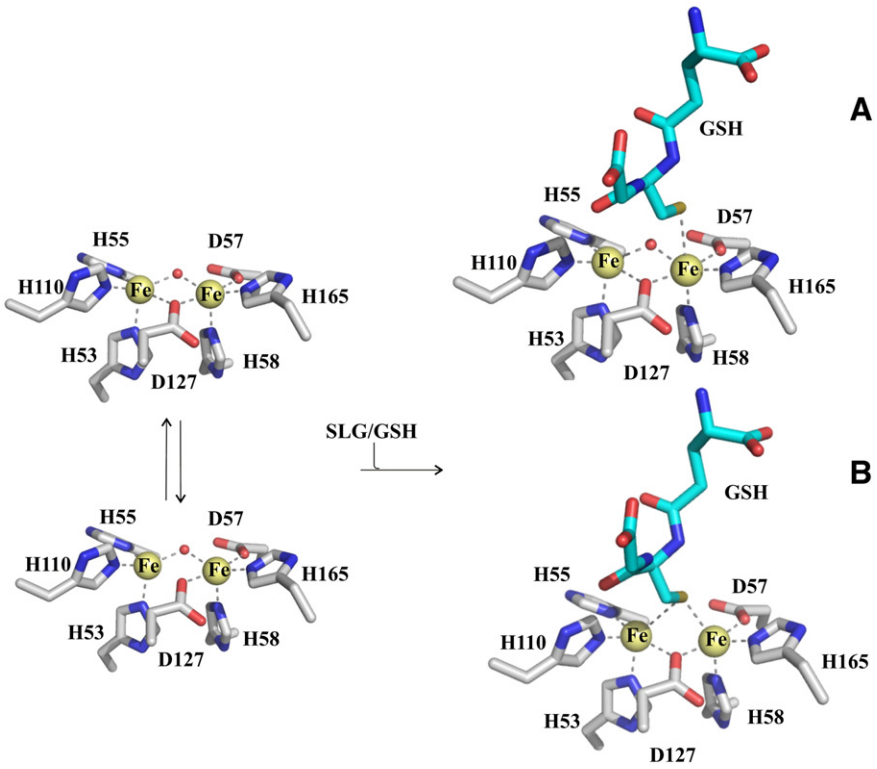

Fig. 5. Cartoon of the active site of GloB during catalysis. The equilibrium between a bridging Asp (left, top) and non-bridging Asp (left, bottom) in the free enzyme is shifted towards the bridged one in the GSH-bound form (right) (A). The thiolate group of glutathione bound to the metal site bridging the two iron ions upon formation of the EP adduct (B).

Abbreviations

GLX	glyoxalase
EPR	electron paramagnetic resonance
RMN	nuclear magnetic resonance
SLG	S-D-lactoylglutathione
GSH	glutathione
E–P	enzyme–product adduct

Acknowledgements

This work was supported by grants from ANPCyT and HHMI to AJV and from PRONEX/FAPESP/CNPq (Grant no 03/09859-2) and CNPq (307102/2006-8) to AJCF. VCB *and JMB are recipients* of fellowships from CONICET. AJV is a Staff member from CONICET and an International Research Scholar of the Howard Hughes Medical Institute. The 600 MHz NMR spectrometer was purchased with funds from ANPCyT (PME2003-0026) and CONICET.

References

[1] G.P. Ferguson, S. Totemeyer, M.J. MacLean, I.R. Booth, Arch. Microbiol. 170 (1998) 209–218.
[2] P.J. Thornalley, Mol. Aspects Med. 14 (1993) 287–371.
[3] B. Mannervik, Drug Metabol. Drug Interact. 23 (2008) 13–27.
[4] P.J. Thornalley, M. Strath, R.J. Wilson, Biochem. Pharmacol. 47 (1994) 418–420.
[5] P.J. Thornalley, Drug Metabol. Drug Interact. 23 (2008) 125–150.
[6] N. Sukdeo, J.F. Honek, Drug Metabol. Drug Interact. 23 (2008) 29–50.
[7] M.W. Crowder, J. Spencer, A.J. Vila, Acc. Chem. Res. 39 (2006) 721–728.
[8] C. Bebrone, Biochem. Pharmacol. 74 (2007) 1686–1701.
[9] D. Liu, P.W. Thomas, J. Momb, Q.Q. Hoang, G.A. Petsko, D. Ringe, W. Fast, Biochemistry 46 (2007) 11789–11799.
[10] P.W. Thomas, E.M. Stone, A.L. Costello, D.L. Tierney, W. Fast, Biochemistry 44 (2005) 7559–7569.
[11] I.L. de la Sierra-Gallay, O. Pellegrini, C. Condon, Nature 433 (2005) 657–661.
[12] C.M. Gomes, C. Frazao, A.V. Xavier, J. LeGall, M. Teixeira, Protein Sci. 11 (2002) 707–712.
[13] C. Frazao, G. Silva, C.M. Gomes, P. Matias, R. Coelho, L. Sieker, S. Macedo, M.Y. Liu, S. Oliveira, M. Teixeira, A.V. Xavier, C. Rodrigues-Pousada, M.A. Carrondo, J. Le Gall, Nat. Struct. Biol. 7 (2000) 1041–1045.
[14] G. Garau, D. Lemaire, T. Vernet, O. Dideberg, A.M. Di Guilmi, J. Biol. Chem. 280 (2005) 28591–28600.
[15] O. Schilling, N. Wenzel, M. Naylor, A. Vogel, M. Crowder, C. Makaroff, W. Meyer-Klaucke, Biochemistry 42 (2003) 11777–11786.
[16] N.F. Wenzel, A.L. Carenbauer, M.P. Pfiester, O. Schilling, W. Meyer-Klaucke, C.A. Makaroff, M.W. Crowder, J. Biol. Inorg. Chem. 9 (2004) 429–438.
[17] T.M. Zang, D.A. Hollman, P.A. Crawford, M.W. Crowder, C.A. Makaroff, J. Biol. Chem. 276 (2001) 4788–4795.
[18] G.P. Marasinghe, I.M. Sander, B. Bennett, G. Periyannan, K.W. Yang, C.A. Makaroff, M.W. Crowder, J. Biol. Chem. 280 (2005) 40668–40675.
[19] V.A. Campos-Bermudez, N.R. Leite, R. Krog, A.J. Costa-Filho, F.C. Soncini, G. Oliva, A.J. Vila, Biochemistry 46 (2007) 11069–11079.
[20] P. Limphong, R.M. McKinney, N.E. Adams, B. Bennett, C.A. Makaroff, T. Gunasekera, M.W. Crowder, Biochemistry 48 (2009) 5426–5434.
[21] A.D. Cameron, M. Ridderstrom, B. Olin, B. Mannervik, Structure 7 (1999) 1067–1078.
[22] S.L. Chen, W.H. Fang, F. Himo, J. Inorg. Biochem. 103 (2009) 274–281.
[23] S.C. Gill, P.H. von Hippel, Anal. Biochem. 182 (1989) 319–326.
[24] T. Inubushi, E.D. Becker, J. Magn. Reson. 51 (1983) 128–133.
[25] I. Bertini, P. Turano, A.J. Vila, Chem. Rev. 93 (1993) 2833–2932.
[26] H.H. Wickman, M.P. Klein, D.A. Shirley, J. Chem. Phys. 43 (1965) 2113–2117.
[27] R.D. Dowsing, J.F. Gibson, J. Chem. Phys. 50 (1969) 294–303.
[28] L. Yu, A. Haddy, F. Rusnak, J. Am. Chem. Soc. 117 (1995) 10147–10148.
[29] W.E. Blumberg, J. Peisach, Ann. N. Y. Acad. Sci. 222 (1973) 539–560.
[30] J. Peisach, W.E. Blumberg, S. Ogawa, E.A. Rachmilewitz, R. Oltzik, J. Biol. Chem. 246 (1971) 3342–3355.
[31] B.G. Fox, M.P. Hendrich, K.K. Surerus, K.K. Andersson, W.A. Froland, J.D. Lipscomb, E. Münck, J. Am. Chem. Soc. 115 (1993) 3688–3701.
[32] B. Guigliarelli, P. Bertrand, J.P. Gayda, J. Chem. Phys. 85 (1986) 1689–1692.
[33] P. Bertrand, B. Guigliarelli, J.P. Gayda, Arch. Biochem. Biophys. 245 (1986) 305–307.
[34] R. Rutter, L.P. Hager, H. Dhonau, M. Hendrich, M. Valentine, P. Debrunner, Biochemistry 23 (1984) 6809–6816.
[35] R.B. Lauffer, B.C. Antanaitis, P. Aisen, L. Que Jr., J. Biol. Chem. 258 (1983) 14212–14218.
[36] E.I. Solomon, S.I. Gorelsky, A. Dey, J. Comput. Chem. 27 (2006) 1415–1428.
[37] S.I. Gorelsky, L. Basumallick, J. Vura-Weis, R. Sarangi, K.O. Hodgson, B. Hedman, K. Fujisawa, E.I. Solomon, Inorg. Chem. 44 (2005) 4947–4960.
[38] M.D. Clay, F.E. Jenney Jr., P.L. Hagedoorn, G.N. George, M.W. Adams, M.K. Johnson, J. Am. Chem. Soc. 124 (2002) 788–805.
[39] S.Y. Gu, X.X. Yan, D.C. Liang, Proteins 72 (2008) 531–536.
[40] H. Daiyasu, K. Osaka, Y. Ishino, H. Toh, FEBS Lett. 503 (2001) 1–6.
[41] J. O'young, N. Sukdeo, J.F. Honek, Arch. Biochem. Biophys. 459 (2007) 20–26.
[42] S. Eriksson, S. Lucchini, A. Thompson, M. Rhen, J.C. Hinton, Mol. Microbiol. 47 (2003) 103–118.
[43] M.L. Zaharik, B.B. Finlay, Front. Biosci. 9 (2004) 1035–1042.
[44] K.M. Papp-Wallace, M.E. Maguire, Annu. Rev. Microbiol. 60 (2006) 187–209.
[45] E. Boyer, I. Bergevin, D. Malo, P. Gros, M.F. Cellier, Infect. Immun. 70 (2002) 6032–6042.